Progress In Electromagnetics Research M, Vol. 93, 137–144, 2020

Contribution to the Experimental Characterization of the Electromagnetic Properties of HTS

Yazid Statra, Hocine Menana*, and Bruno Douine

Abstract—This work is a contribution to the characterization of the electromagnetic properties of high temperature superconductors (HTS) made of Bismuth Strontium Calcium Copper Oxides (BSCCO). The electromagnetic proprieties (critical current density and self-field AC losses) of a tape and a coil are determined experimentally at different frequencies, and compared to analytical models and finite element simulations for a better analysis of the physical phenomena. As shown in this work, the transition from the element to the system is not straightforward, and the characterization of such a material at the system scale is necessary due to their high sensitivity to the magnetic field. Solutions to some measurement problems are also highlighted.

1. INTRODUCTION

Superconducting materials present extraordinary electromagnetic properties [1]. Since their discovery in 1911, research on these materials evolves on both the theoretical aspects to understand the physical phenomena and their applications, especially after the discovery of high temperature superconductors (HTS). However, the integration of HTS in power systems remains very limited, particularly in AC electrical machines, where their use is generally restricted to the function of inductors in synchronous machines [2]. The reasons for that are not only related to the technical constraints of realization, but also related to the high sensitivity of such materials to their electromagnetic environment. Even if a lot of work has been done on the characterization of superconducting elements (bulks, tapes...) [3–5], the transition from the element to the system is not obvious, because the behavior of an isolated HTS element is very different when it is integrated into a system. In this context, in this work, the electromagnetic proprieties (critical current density and AC self-field losses) of samples and coils, made of BSCCO type tapes, are determined experimentally at different frequencies, and compared to analytical models [5] and finite element simulations, where the electrical properties of the HTS are represented by the power law combined with the Kim's law to take into account the dependence of the critical current with the magnetic field.

The experimental characterization procedures are described in the next section, followed with results and discussions presented in the last section.

2. CHARACTERIZATION METHODS

2.1. Experimental Characterization of the $E(J)$ Relation

Assuming that the current density is homogeneously distributed in the section of the characterized element, the $E(J)$ characteristic is deduced from the measurement of the $U(I)$ curve of the HTS element (tape sample or coil) by using the four-point method [2]. It consists of supplying the superconducting

Received 7 May 2020, Accepted 10 June 2020, Scheduled 18 June 2020
* Corresponding author: Hocine Menana (hocine.menana@univ-lorraine.fr).
The authors are with the Université de Lorraine, GREEN, F-54000 Nancy, France.

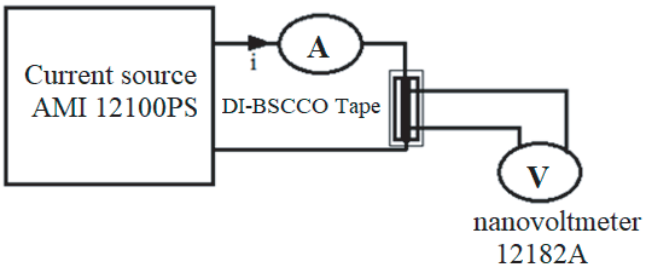

Figure 1. Experimental setup for the $E(J)$ curve characterisation.

element by a DC current source (I), and then the voltage drop (U) over the element's terminals is measured by mean of a nanovoltmeter as shown in Fig. 1. The critical value of the electric field (E_c) is set to 1 μV/cm. The critical voltage (U_c) of the element is the product of E_c by the tape length between the potential measurement points. The critical current (I_c) is the magnitude of the supplying current giving a voltage drop $U = U_c$.

2.2. AC Losses Measurement

The experimental setup for AC losses measurement, using a synchronous detection voltmeter, is shown in Fig. 2 [6]. The superconducting element (tape or coil) is supplied by a sinusoidal current provided by an AC current source of variable amplitude and frequency. The measured voltage at the element's terminals is composed of two parts: an inductive part and a resistive part which is responsible of the power losses. The first part is several hundred times higher than the second one. If the measuring device is calibrated for this voltage level, the resistive part would be embedded in its error's margin, which would lead to significant measurement errors of this part. To overcome this constraint, the measurement of the inductive part is compensated. A compensating coil is added in series with the measuring circuit and placed close to the supply cable (Fig. 2). The coil is oriented such as its mutual inductance with the power cable opposes the inductance of the measuring element (tape or coil). The measured voltage is then expressed as follows:

$$U(t) = U_{losses}(t) + (L - M)\frac{di(t)}{dt} \tag{1}$$

The distance between the compensating coil and the power cable is varied so that the value of the mutual inductance M approaches to the self-inductance (L) of the superconducting sample. It is not necessary to completely eliminate the inductive part, but to reduce it to a value close to that of the resistive part.

The current signal is used as a reference in the synchronous detection voltmeter. The measured voltage is non-sinusoidal because of the nonlinear behavior of the HTS. Only the fundamental of this voltage contributes to the AC losses. It should be noted that the measurement at the network frequency

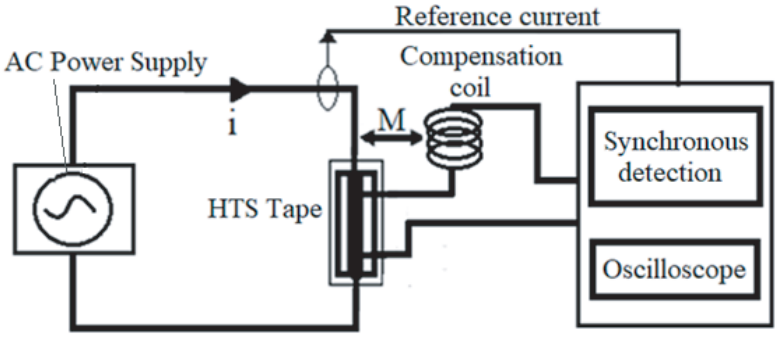

Figure 2. AC losses measurement setup.

(50 Hz) is to be avoided because it is generally very disturbed by the surrounding equipment powered at this frequency.

3. RESULTS AND DISCUSSIONS

A HTS tape made from non-insulated DI-BSCCO (Dramatically Innovative Bismuth Strontium Calcium Copper Oxide) manufactured by Sumitomo electric (ACT type) in 2011 is used [7]. The coil is wound by a fully insulated tape. The tape and coil specifications are listed in Table 1. All the measurements were carried out at 77 K, in liquid nitrogen.

Table 1. Tape and coil specifications.

Tape		**Coil**	
Width	2.8 mm	Inner radius	25 mm
Thickness	0.33 mm	Outer radius	50 mm
Section	0.93 mm^2	Number of turns	63
Distance between the voltage taps	20 cm	Distance between the voltage taps	14.8 m

3.1. The $E(J)$ Curves

The measured $U(I)$ curves for the tape and coil are shown in Fig. 3. The determined critical current of the tape is 69.5 A, while that of the coil is about 44 A. This degradation is due to the influence of the coil's magnetic field on the HTS tape. Indeed, the behavior obeys to a power law expressed by Eq. (2), in which the critical current (I_c) and the creep exponent (n) strongly depend on the intensity of the magnetic field and its orientation (Eqs. (3) and (4)) [8–10]. As a result, the shape of a superconducting coil directly affects its electromagnetic performances. In Eqs. (3) and (4), n_0 and I_{c0} represent respectively the values of the zero field creep exponent and critical current; $B_{\|}$ and $B_{\perp}$ represent the components of the magnetic field parallel and perpendicular to the tape width, and k, β, B_{J0} and B_{n0} are constants characterizing the material used.

$$U(I) = U_C \left(\frac{I}{I_C(B)} \right)^{n(B)} \tag{2}$$

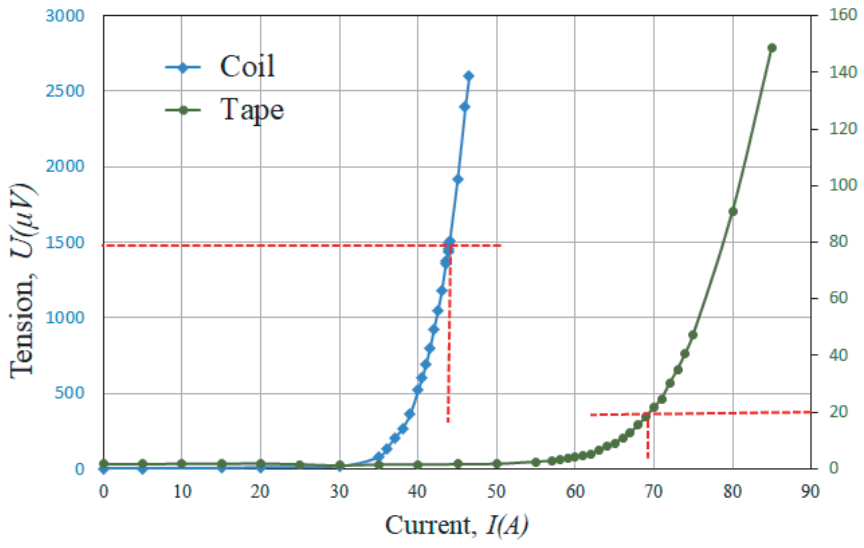

Figure 3. Measured $U(I)$ curves in the tape and coil in DC conditions.

$$I_C = \frac{I_{c0}}{\left(1 + B_{J0}^{-1}\sqrt{k^2 B_\parallel^2 + B_\perp^2}\right)^\beta} \tag{3}$$

$$n = \frac{n_0}{\left(1 + B_{n0}^{-1}\sqrt{k^2 B_\parallel^2 + B_\perp^2}\right)} \tag{4}$$

3.2. AC Losses

The tested element is supplied by a sinusoidal current with variable amplitude $I_{\max}$. The AC losses measured in the tape at different frequencies are plotted in Fig. 4 as function of the ratio ($i = I_{\max}/I_c$). For comparison, the losses given by the Norris formulas for tapes of elliptical and strip sections [5], expressed, per cycle and per unit length in Eqs. (4) and (5), are also plotted in Fig. 4.

$$Q_{sfe} = \left(\mu_0 I_c^2/\pi\right)\left[(1-i)\ln(1-i) + (2-i)\,i/2\right] \tag{5}$$

$$Q_{sfs} = \left(\mu_0 I_c^2/\pi\right)\left[\begin{array}{c}(1-i)\ln(1-i)\\ +(1+i)\ln(1+i) - i^2\end{array}\right] \tag{6}$$

As shown in Fig. 4, the AC losses for the considered frequencies fall between the Norris elliptical and strip curves. At low frequencies, the measured losses are close to those calculated for an elliptical section (Eq. (4)), and as the frequency increases, the measured losses fall more closely to the Norris strip curve (Eq. (5)).

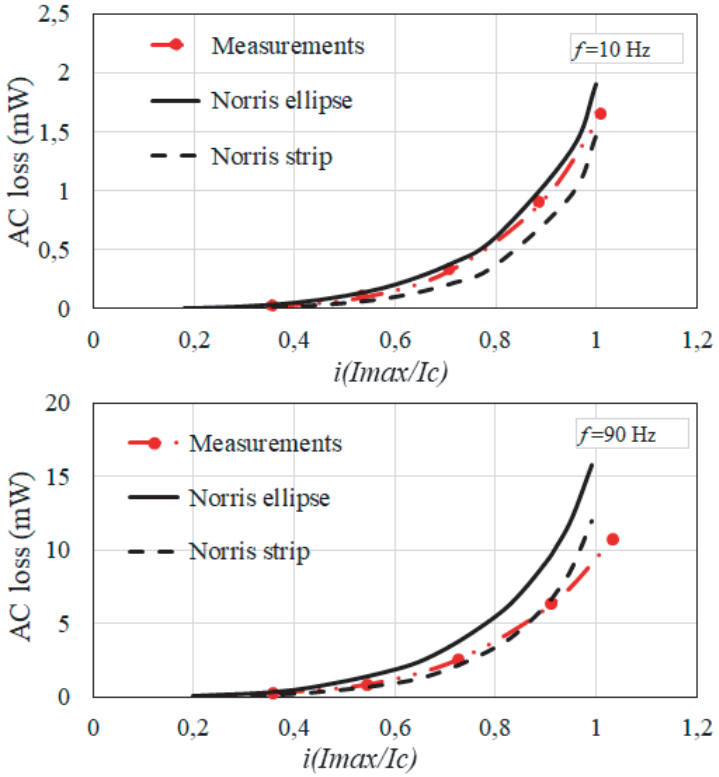

Figure 4. Self-field AC losses in the tape as a function of the current ratio i for two frequencies: 10 Hz and 90 Hz.

The self-field AC losses per cycle decrease with frequency as shown in Fig. 5 which represents the measured losses normalized to $\mu_0 I_c^2 f/\pi$. The physical aspects behind are well described in the literature [11]. This evolution of the losses per cycle with the frequency is not predicted by the Norris model. In order to quantify this evolution, we have implemented on COMSOL software a finite element

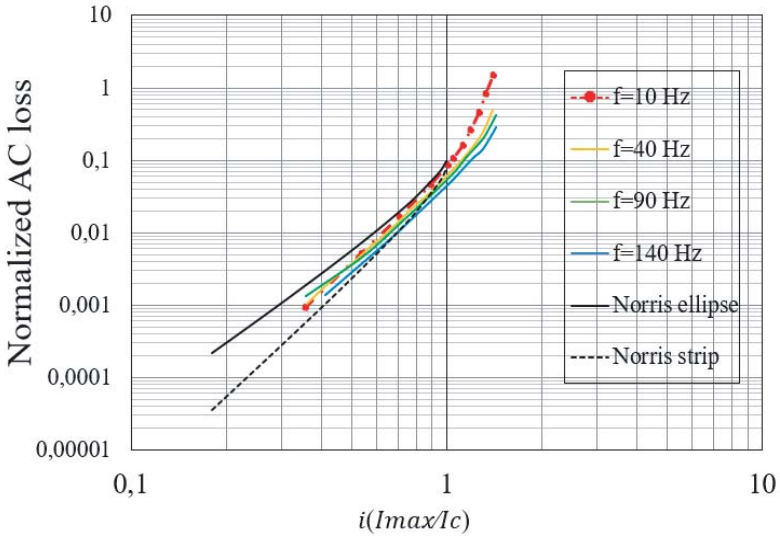

Figure 5. Normalized self-field AC losses of the tape as a function of the current ratio i for different frequencies.

modelbased on the H-formulation [12], where the power law is used to represent the $E(J)$ characteristic of the HTS, with the use of the Kim's model to take into account the variation of the critical current with the magnetic field: $J_c(B)$. The H-formulation is given as follows:

$$\begin{cases} \vec{\nabla} \times \left(\rho(J) \vec{\nabla} \times \vec{H} \right) + \mu_0 \partial_t \vec{H} = 0 \\ \rho\left(J\right) = E_c J_c^{-1} (J_c^{-1} J)^{n-1} \end{cases} \tag{7}$$

where ρ, μ_0, and H are the resistivity, vacuum permeability, and magnetic field, respectively. The simulations were performed in 2D time domain.

The critical current density J_c is determined from the measured critical current considering only the section of the superconducting material which represents 30% of the total section of the tape (matrix + superconductor). The AC losses are calculated on two periods of the applied current, and the mean losses in the second period are compared to the measurements.

The parameters involved in Eqs. (3) and (4) are difficult to identify, in particular in self-magnetic fields [13]. In this work, these parameters have been determined in such a way that the calculated losses match the measured losses for a frequency of 10 Hz. The chosen parameters are listed in the Table 2. Using these parameter, a good agreement is also found between simulations and measurements for the other frequencies as shown in Fig. 6.

Table 2. Used parameters for the Kim's model.

Parameter	J_{c0}	B_{J0}	k	β	n_0	B_{n0}
Tape	360.75 A/mm^2	0.018 T	0.14	2.9	11	0
Coil	207.94 A/mm^2	0.14 T	0.14	2.28	11	59.7 mT

As mentioned above, due to the strong dependence of the electromagnetic properties of HTS on the magnetic field, the behavior of an HTS element is very different when it is integrated into a system. This is illustrated in Fig. 7 which shows a comparison at 10 Hz between the measured self-field AC losses of the HTS coil and the self-field AC losses of a straight HTS tape of length equal to that of the coil wire. The tape losses are obtained by multiplying the measured losses per unit length by the tape length. The significant difference between the results is due to the influence of the magnetic field which considerably affects the performances of the HTS tape. This has to be taken into account when sizing HTS coils.

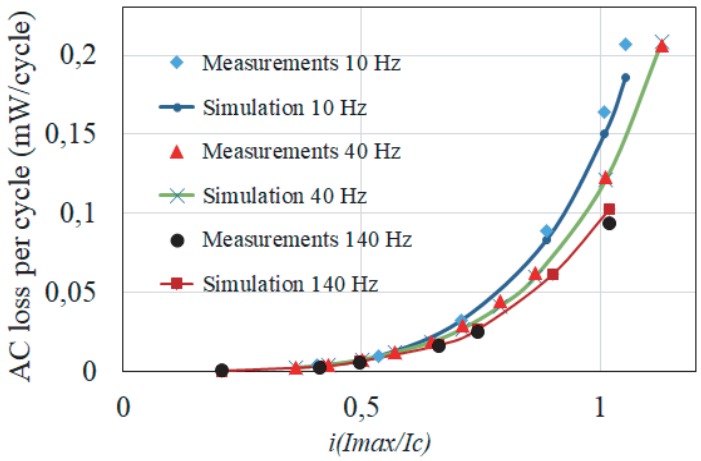

Figure 6. Comparison between the simulated and measured self-field AC losses per cycle in the tape.

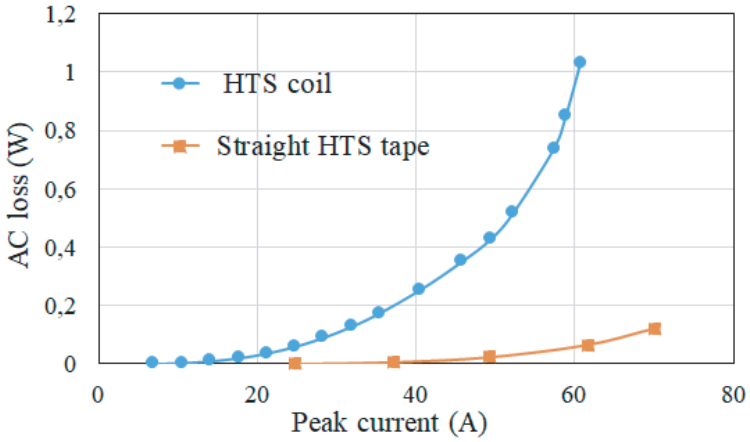

Figure 7. Comparison of the measured self-field AC losses in the coil with those calculated in a straight tape of the same length ($f = 10\,\text{Hz}$).

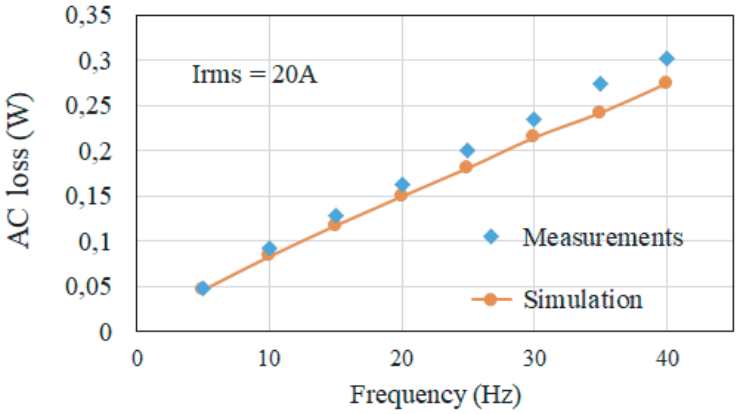

Figure 8. Self-field AC losses in the coil as a function of frequency.

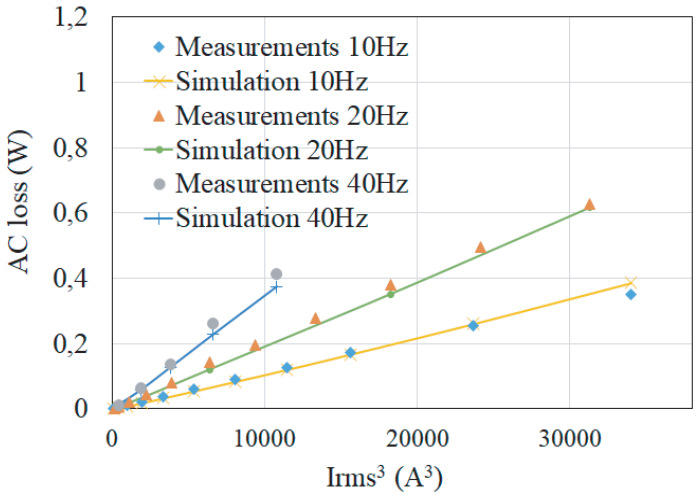

Figure 9. Self-field AC losses in the coil as a function of cubed current.

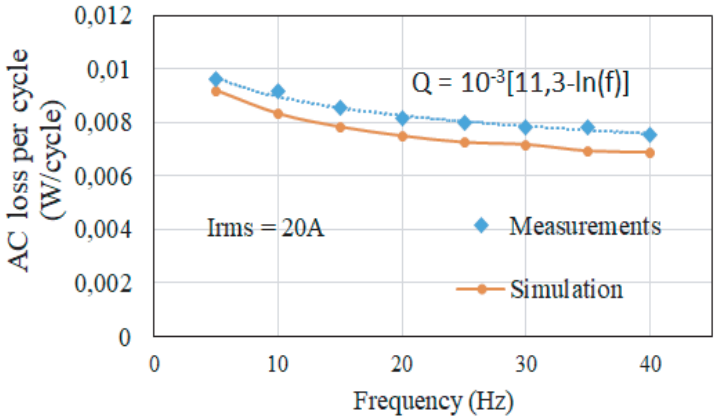

Figure 10. Self-field AC losses per cycle in the coil as a function of frequency.

2D axisymmetric finite element simulations were also performed for the HTS coil, with a bulk approximation of its section. The parameters given in [7] were used in the Kim's model. These parameters are listed in Table 2, where J_{c0} takes into account the volume fraction of the HTS in the coil section. Simulations results and measurements are in a good agreement as shown in Figs. 8 and 9. We also notice that the losses are proportional to the frequency and the cubed current (I^3). It means that in AC regimes, the hysteresis losses in HTS are predominant in self-field (i.e., no external magnetic field applied). As for the tape, the self-field AC losses per cycle decrease as the frequency grows which is shown in Fig. 10. This decrease follows a logarithm dependency on the frequency for both measurements and simulations.

4. CONCLUSION

In this work, DI-BISCCO/Ag-sheathed HTS materials have been characterized as sample (tape) and system (coil). The study shows the necessary of a characterization of such materials at the system scale due to their high sensitivity to the magnetic field. Solutions to some measurements issues are also provided. The good agreement between the simulation and the measurements shows that the models used are quite realistic and representative of the physical phenomena at the considered frequencies.Reliable modeling and experimental results are provided which could be used further for models validation or HTS systems design and optimization.

REFERENCES

1. Tixador, P., *Les Supraconducteurs*, Hermès Science, 1995.
2. Bendali, S., "Dimensionnement d'un moteur supraconducteur HTc," Ph.D. thesis, Lorraine University, 2012.
3. Gianni, L., et al., "Transport ac losses in YBCO coated conductors," *IEEE Trans. Appl. Superconduct.*, Vol. 16, No. 2, 147–149, Jun. 2006.
4. Campbell, A. M., "A general treatment of losses in multifilamentary superconductors," *Cryogenics*, Vol. 22, 3–16, 1982.
5. Norris, W. T., "Calculation of hysteresis losses in hard superconductors carrying as: Isolated conductors and edges of thin sheets," *Journal of Physics D*, Vol. 3, 489–507, 1970.
6. Douine, B., J. Lévêque, and A. Rezzoug, "AC losses measurements of a high critical superconductor transporting sinusoidal or non sinusoidal current," *IEEE Trans. Appl. Superconduct.*, Vol. 10, No. 1, 1489–1492, Mar. 2000.
7. SUMITOMO, http://www.sei.co.jp/super/hts/.
8. Kim, Y. B., C. F. Hempstead, and A. R. Strnad, "Critical persistent currents in hard superconductors," *Physical Review Letters*, Vol. 9, No. 7, 306–309, Oct. 1962.
9. Grilli, F., F. Sirois, V. Zermeño, and M. Vojenciak, "Self-consistent modeling of the Icof HTS devices: How accurate do models really need to be?," *IEEE Trans. Appl. Superconduct.*, Vol. 24, No. 6, 1–8, 2014.
10. Willis, J. O., J. Y. Coulter, and M. W. Rupich, "n-value analysis of position-dependent property variability in long-length coated conductors," *IEEE Trans. Appl. Superconduct.*, Vol. 21, No. 3, 2988–2991, 2011.
11. Thakur, K. P., A. Raj, E. H. Brandt, J. Kvitkovic, and S. V. Pamidi, "Frequency-dependent critical current and transport ac loss of superconductor strip and Roebel cable," *Supercond. Sci. Technol.*, Vol. 24, No. 6, 2011.
12. Brambilla, R., F. Grilli, and L. Martini, "Development of an edge element model for Ac loss computation in high temperature superconductors," *Supercond. Sci. Technol.*, Vol. 20, 16–24, 2007.
13. Douine, B., et al., "Self field effect compensation in an HTS tube," *IEEE Trans. Appl. Superconduct.*, Vol. 18, No. 3, 1698–1703, 2008.